

## Nitrogen states in Ga(As,P) and the intermediate-range model

George G. Kleiman

*Instituto de Física, Universidade Estadual de Campinas, 13100 Campinas, São Paulo, Brasil*

(Received 18 August 1978)

The appearance of new single nitrogen lines in recent Ga(As,P):N photoluminescence data has been interpreted theoretically in terms of an impurity potential that has a short-range part and a more extended portion arising from strain effects. Two current theories have interpreted the range of the latter as either long or intermediate: the implications for impurity-induced lattice relaxation are quite different in the two cases. To resolve this issue, we examine the consistency of the data with a nearest-neighbor shell model as well as with more extended intermediate-range models. By introducing a soluble Green's-function model, we show that the former is inconsistent; from basic quantum-mechanical considerations, we show that monotonic, attractive potentials are not consistent unless their ranges are greater than  $\sim 20\text{--}25 \text{ \AA}$ .

### I. INTRODUCTION

The strong luminescence of the isoelectric impurity nitrogen in indirect III-V mixed-crystal semiconductor alloys containing phosphorus [principally Ga(As, P):N] is of considerable practical interest in the fabrication of light-emitting diodes.<sup>1</sup> Until recently, luminescence measurements of Ga(As, P):N were interpreted within the traditional picture in which the nitrogen electronic potential  $V_s$  is concentrated in the impurity's central cell and is presumed to arise from the difference in core electronic structure between nitrogen and phosphorus.<sup>1,2</sup>

The physical consequences of this picture have been calculated<sup>3-12</sup> within the one-band one-site Koster-Slater model.<sup>13</sup> In contrast to the case of long-range (e.g., hydrogenic) impurity potentials, this model predicts only one nitrogen electronic state whose eigenstate has components from all points in  $\vec{k}$  space within the first Brillouin zone (in agreement with the Heisenberg uncertainty principle).<sup>1,2</sup> These components are completely described in terms of conduction-band parameters (except for the Koster-Slater potential parameter,  $V_0 \equiv \langle \vec{R}_0, c | V_s | \vec{R}_0, c \rangle$ , where  $|\vec{R}_0, c\rangle$  is a conduction-band Wannier state centered at the nitrogen position,  $\vec{R}_0$ ) and are proportional to  $[E_N - E_c(\vec{k})]^{-1}$ , where  $E_N$  is the energy of the bound nitrogen state and  $E_c(\vec{k})$  is the conduction-band dispersion relation. Therefore, the localized impurity state has strong  $\vec{k}=0$  components (and, consequently, luminescence) even in indirect crystals and this luminescence increases as  $E_N \rightarrow E_c(\vec{k}=0) \equiv E_\Gamma$ , where  $\Gamma$  denotes  $\Gamma_6^c$ , the central conduction-band minimum (this increase embodies the phenomenon of band-structure enhancement, or BSE<sup>2</sup>).

Recent data<sup>14-16</sup> present evidence in support of a more extended potential model of nitrogen in the

ternary alloy. Spectra which had been associated<sup>1,17,18</sup> with pairs of nitrogen atoms (in analogy with the case of GaP<sup>2</sup>) were shown to be probably phonon sidebands of single nitrogen lines.<sup>14</sup> In addition, more than one single nitrogen line has been identified.<sup>15,16</sup> For  $x \lesssim 0.30$ , where  $x$  is the mole fraction of P, the lower of these lines  $N_x$  appears<sup>19</sup> to run parallel to  $E_\Gamma$ , while for  $x \gtrsim 0.30$ ,  $N_x$  seems to behave like the Koster-Slater state already described (i.e., its binding energy,  $E_x - E_{N_x}$  where  $E_x$  is the energy of the conduction-band minimum at  $X_6^c$ , or  $X$ , increases with increasing As content) and seems to be associated with  $X$ .<sup>16</sup>

The next higher state  $N_\Gamma$  has more complex behavior. For  $x \lesssim 0.30$ , it approaches  $E_\Gamma$  and appears to become resonant for  $x \approx 0.28$ ; for  $0.30 \lesssim x \lesssim 0.42$ , it seems to follow  $E_\Gamma$ ; and for  $0.42 \lesssim x \lesssim 0.47$  it seems to parallel  $E_x$ . These conclusions are supported by pressure-dependent photoluminescence measurements. Finally, for  $x \gtrsim 0.47$ ,  $N_\Gamma$  seems to disappear.

Photoluminescence data for as-grown Ga(As,P):N are illustrated in Fig. 1.<sup>20,21</sup> In addition to the two states discussed above, these data manifest the existence of a third state<sup>20</sup>  $N'_\Gamma$  which had been predicted theoretically.<sup>19,22</sup> Corresponding data<sup>23</sup> for samples in which nitrogen ions are implanted seem to show no evidence of  $N'_\Gamma$ . These discrepancies may be a result of the difference between as-grown and ion-implanted material.

Two features of *all* of the data serve to illustrate the rather subtle issues involved in theoretical interpretation: (i) One of the states,  $N_x$ , follows  $X$  and another,  $N_\Gamma$ , follows  $\Gamma$  (at least for  $0.30 \lesssim x \lesssim 0.42$ ) and (ii)  $N_x$  is strongly luminescent throughout the entire range of  $x$ . It has been suggested<sup>15</sup> that the nitrogen potential produces two states describable within the effective mass approximation,<sup>24</sup> one ( $N_\Gamma$ ) associated with  $\Gamma$  and the other ( $N_x$ ) with

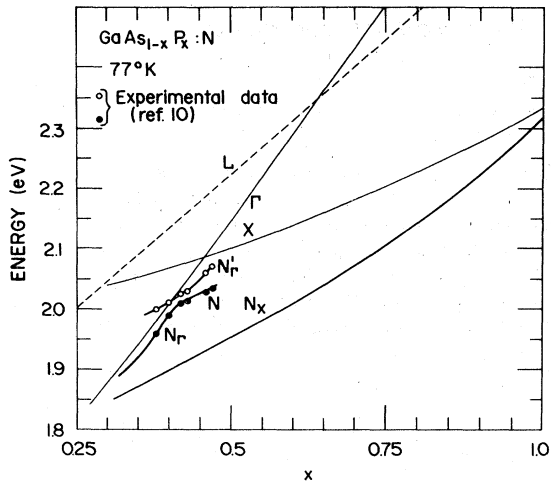


FIG. 1. Photoluminescence data indicating the concentration dependence of  $\Gamma$ ,  $L$ ,  $X$  and the peaks associated with electronic states of isolated nitrogen impurities in Ga(As,P) (after Refs. 20 and 21).

$X$ : Such a model describes feature (i) nicely. In fact, the potential radius extracted from the data<sup>15</sup> ( $=3+40x$  Å) is well in concert with the usual type of long-range potential used in the effective-mass approximation (i.e., the wave functions exhibit the same order of localization). Unfortunately, this approximation also predicts<sup>25</sup> that  $N_X$  would be well-localized about  $X$  in  $\vec{k}$  space, in disagreement with feature (ii). It is clear, therefore, that any theoretical description must involve both a short-range and a more extended part.

Two theoretical proposals based upon extended nitrogen potentials have been made to describe this data.<sup>19,22,23</sup> The first of these<sup>19,22</sup> attributes a long-range potential  $V_l$ , as well as the conventional short-range potential  $V_s$  to the nitrogen. The long-range potential is presumed to arise from deformation of the lattice induced by strains associated with the presence of nitrogen. To account for the data, the only property which is required of  $V_l$  is that it be strong enough to bind one state associated with  $X$  and one with  $\Gamma$ ; the short-range potential  $V_s$  is presumed to produce a bound state which is delocalized in  $\vec{k}$  space as in the conventional Koster-Slater picture. Since the observed lines are associated with eigenfunctions corresponding to  $V = V_l + V_s$ , the predictions of the theory can be interpreted<sup>19,22</sup> as arising from hybridization of the states associated with  $V_l$  and  $V_s$  separately and result from the *intrinsic nature of  $V$*  independent of specific values of potential parameters. These predictions are in agreement with all the general features of the data; that is, the theoretical energies display the same general  $x$  dependences as the experimental data in Fig. 1. Indeed,

numerical calculations<sup>22,26</sup> show that a good absolute agreement with available data<sup>14-16,19,20,23,27,28</sup> can be achieved. The potential parameters which are extracted are consistent with fundamental considerations; for example, the radius of  $V_l \sim 20-25$  Å, which is in accord with the long-range nature of  $V_l$  (i.e., the validity of the effective-mass approximation).

One of the general predictions of this theory is the existence of the highest state  $N'_\Gamma$  shown in Fig. 1. Although the theory is semiphenomenological in the sense that the exact values of the potential parameters are determined from experiment (so that lack of observation of  $N'_\Gamma$  could be explained by its being a resonant, or unbound state not in the gap) clarification of the above-mentioned discrepancy between data for as-grown<sup>20</sup> and for nitrogen-implanted<sup>23</sup> samples would help to determine the validity of this theory.

A later model was suggested<sup>23</sup> to explain the data for nitrogen-implanted specimens. This model also associates the nitrogen impurity with an extended potential. Here, however, the potential consists of an intermediate-range extended part  $V_i$  as well as the short-range part  $V_s$ . More specifically, the strain field is presumed to induce an attractive impurity potential in the first shell of nitrogen nearest neighbors as well as at the nitrogen site. This model predicts *two* symmetric states (i.e., with high  $\vec{k}=0$  probability amplitudes) whose energies are fitted independently to  $N_\Gamma$  and  $N_X$  near  $x \approx 0.35$  after some simplifications in the calculations reported.<sup>23</sup> The limited range of the potential causes neither of these states to be localized in  $\vec{k}$  space about a conduction band minimum. The association of one state with  $\Gamma$  and the other with  $X$  is, therefore, a result of fitting the data and is not an intrinsic consequence of the model<sup>23</sup> as in the Kleiman theory.<sup>19,22</sup>

Although this model<sup>23</sup> cannot reproduce some of the features in the data, such as the curvature in  $E_{N_\Gamma}$  for  $x \sim 0.45$  and in  $E_{N_X}$  for  $x \sim 0.30$ , the predictions are in reasonable agreement with luminescence strength<sup>23</sup> and lifetime<sup>28</sup> measurements as well as with the observed energies for  $0.28 \leq x \leq 0.40$ .

It would seem at this juncture that there is little to distinguish the predictions of the intermediate-range<sup>23</sup> from those of the long-range model<sup>19,22</sup> except the existence of the third state  $N'_\Gamma$ <sup>20</sup> (which has not been observed in nitrogen-implanted material<sup>23</sup>) and the curvatures in  $E_{N_\Gamma}$  and  $E_{N_X}$  (which could be explicable, at least partially, in terms of bound-exciton valley-valley interactions). Although electromodulation spectroscopy<sup>29,30</sup> indicates the existence of two states for  $x \geq 0.55$  (in support of the long-range, or Kleiman theory), there would

appear to be sufficient uncertainty to fuel a controversy over the validity of the two models.

That it is important to resolve this question is clear from the point of view of understanding the nature of the nitrogen potential in Ga(As, P) and other III-V alloys. That it is more fundamentally and generally important is, perhaps, not so clear. In the intermediate-range model,<sup>23</sup> the strain-induced potential is large in a small region surrounding the impurity and dies away rapidly with distance: This picture is entirely in agreement with conventional intuition regarding impurity-induced lattice relaxation in semiconductors. In the long-range theory, on the other hand, the potential is associated with a large region (i.e., of radius 20–25 Å), a relaxation of such magnitude is unexpected. Should the long-range model prove to be correct in its essentials, therefore, it would suggest important consequences for other impurities in other semiconductors.

In order to clarify this situation, this article addresses the problem of the consistency of intermediate-range models with photoluminescence measurements of nitrogen-derived line (i.e.,  $N_\Gamma$  and  $N_X$ ) energies in Ga(As, P):N.<sup>14-16, 19, 20, 23</sup> The fundamental nature of the question involved makes it preferable to generalize the definition of the intermediate-range model, rather than restrict it to the specific case already treated in Ga(As, P):N.<sup>23</sup> To this end, we posit that such models are those in which the range of the potential is fixed to be less than the minimum needed to localize an impurity  $\vec{k}$ -space wave function about a conduction-band minimum but in which the strength of the potential can be varied to describe the data.

We have seen that long-range potentials whose binding energies agree with the experimental energies<sup>14-16, 19, 20, 23</sup> can be found.<sup>15, 22, 23</sup> Can intermediate-range models be found which manifest similar agreement? The results of this paper indicate a negative answer to this question.

This result follows from the fact that specifying part of the bound-state energy spectrum [even two states, as in the case of Ga(As, P):N] imposes a severe restriction upon the potential producing these states. In illustration, consider two states of different energies corresponding to masses  $m_\Gamma$  and  $m_X$  (i.e.,  $m_\Gamma < m_X$ ) in the effective-mass approximation.<sup>24</sup> For a square-well potential, the values of these energies determine the depth and range of the potential *uniquely*<sup>19, 22</sup>: In the case of nitrogen in Ga(As, P), the range ~20–25 Å.<sup>22, 23</sup> In passing, it is interesting to observe that, of all the monotonically increasing spherically symmetric attractive potentials (i.e., whose minimum is at  $r=0$ ) of finite range which produce two such given energies, the square-well corresponds to the

*smallest* range.

By fixing the range and allowing only the strength of the potential to vary, therefore, one cannot, in general, reproduce states of given energies unless the range is sufficiently long. Although we applied these arguments to potentials for which the effective-mass approximation holds, they are more generally true. In Sec. IIA, we discuss an impurity potential restricted to the nitrogen cell and the first shell of 12-nearest-neighbor cells surrounding it.<sup>23</sup> In this situation, the effective-mass approximation is not valid. Nevertheless, we show that this model is not consistent with the Ga(As, P):N data, the reason being (in the language of the effective-mass approximation) that the range is insufficient. More specifically, if we fix the value of the energy of one of the two lowest states at the experimental value  $E_{N_X}$  then we cannot find a set of potential parameters which give  $E_{N_\Gamma}$  for the other energy.

The energies of these states depend upon the conduction-band structure through the Wannier-representation Green's-function matrix elements, as the effective-mass energies depend upon the band structure through the masses,  $m_\Gamma$  and  $m_X$ . Because of the limited range of the potential, *all* of the  $\vec{k}$ -space band structure is represented. By forcing the  $N_X$  state to follow the  $X$  minimum through fitting to the experimental energies  $E_{N_X}$ , the potential parameters derived thereby contain the influence of the large density of states associated with this minimum.<sup>3-12</sup> Since the higher state is not independent,<sup>31</sup> its energy is influenced by  $X$  through these parameters and it cannot be made to follow  $\Gamma$  (i.e., fit to the experimental energy  $E_{N_\Gamma}$ ).

The influence of all the minima upon both states can, therefore, be seen to be a consequence of the local nature of the impurity potential. As more cells are included within the range of the impurity potential, the relevant matrix elements of the Green's function become more local in  $\vec{k}$  space. In order to describe the experimental energies, therefore, we must have a potential of sufficient range that the  $\Gamma$  and  $X$  minima are decoupled. This condition resembles that necessary for the effective-mass approximation to hold. Since the effective-mass approximation can be derived as a limiting case if enough sites are included within the range of the impurity potential, it would seem that long-range potentials are the only ones consistent with the data. We discuss this point in more detail in Sec. IIB.

The conclusions are presented in Sec. III. The first of these is that the Ga(As, P):N energy data<sup>14-16, 18, 23, 27</sup> is inconsistent with the extended Koster-Slater model used previously<sup>23</sup> as well as with more general versions of the intermediate-

range model potential. We are, therefore, left with a long-range potential as the only semiempirical model capable of describing the data. The strong luminescence of both  $N_T$  and  $N_X$  require a short-range core to the potential.

In this work, we have followed the conventional<sup>3-12</sup> point of view that bands other than the lowest conduction band do not contribute to the short-range nitrogen potential matrix elements. Inclusion of such contributions might modify some of our conclusions. In the absence of convergent first-principles calculations, however, such effects are poorly understood.<sup>32</sup> In any case, our conclusions are valid within the context of semiempirical models for which coupling to only the lowest conduction band is considered.<sup>22, 23</sup>

## II. CONSISTENCY OF INTERMEDIATE-RANGE MODELS

In this section, we examine critically the possibility that the photoluminescence data<sup>14-16, 19, 20, 23, 27, 28</sup> in Ga(As, P):N are consistent with model potentials of range insufficient to localize the resultant states in  $\vec{k}$  space (i.e., intermediate range models, according to the definition in Sec. I). In Sec. IIA, we demonstrate that a model involving attractive potentials localized in the nitrogen cell and in the first shell of nearest-neighbor cells (i.e., this model includes the extended Koster-Slater model used previously<sup>23</sup>) cannot be fit to the energy data.<sup>14-16, 20, 23</sup> Section IIB contains arguments extending these results to more general semiempirical intermediate-range model potentials.<sup>33</sup>

### A. Nearest-neighbor shell models

In this part, we consider impurity potentials  $V$ , which involve only the nitrogen site,  $\vec{R}_0=0$ , and the first shell of its nearest-neighbor cells. We demonstrate that such potentials cannot give rise to the experimentally observed states in Ga(As, P):N.

The coefficients of an impurity state  $|j\rangle$  (in the Dirac notation) expanded in the complete set of Wannier states  $|\vec{R}_I, n\rangle$  corresponding to site  $\vec{R}_I$  and band  $n$  are given in the following equations<sup>34</sup>:

$$|j\rangle = \sum_{I, n} |\vec{R}_I, n\rangle \langle \vec{R}_I, n | j \rangle, \quad (1a)$$

$$\begin{aligned} \langle \vec{R}_I, n | j \rangle &= \sum_{I, J, M} G_{0n}(\vec{R}_I, \vec{R}_J, E_j) \\ &\quad \times \langle \vec{R}_I, n | V | \vec{R}_J, M \rangle \langle \vec{R}_J, M | j \rangle, \end{aligned} \quad (1b)$$

$$\begin{aligned} G_{0n}(\vec{R}, \vec{R}', E) &\equiv \langle \vec{R}, n | G_0(E) | \vec{R}', n \rangle \\ &= \frac{1}{N_0} \sum_{\vec{k}} \frac{e^{i\vec{k} \cdot (\vec{R} - \vec{R}')}}{E - E_n(\vec{k}) + i\delta}, \end{aligned} \quad (1c)$$

$$G_0(E) \equiv (E + i\delta - H_0)^{-1}. \quad (1d)$$

In Eqs. (1), the symbols  $E_j$ ,  $N_0$ , and  $E_n(\vec{k})$  denote, respectively, the energy eigenvalue of  $|j\rangle$ , the number of unit cells in the pure host crystal, and the  $\vec{k}$ -space energy dispersion relation of the  $n$  band [i.e., the sum in Eq. (1c) is restricted to the first Brillouin zone]. The quantity  $G_{0n}$  represents the pure-crystal Green's function of the  $n$  band in the Wannier representation.<sup>34</sup> Because of the limited range of the potentials which we consider in this section, this representation is more appropriate than that in terms of Bloch waves. The symbol  $H_0$  denotes the pure-crystal Hamiltonian and  $\delta \rightarrow 0^+$ .

Although Eqs. (1) show explicitly that coupling between bands is involved and is expected<sup>25</sup> to be important in the case of potentials of limited range, definitive calculation of the effects of such coupling has not yet been achieved.<sup>32</sup> We follow, instead, the semiempirical point of view, which is the traditional one applied to the problem.<sup>3-12, 19, 22, 23</sup> In this picture,  $V$  is assumed to have no interband matrix elements. The corresponding equation for the coefficients of the lowest conduction band,  $c$ , is, therefore

$$\begin{aligned} \langle \vec{R}_I, c | j \rangle &= \sum_{I, J} G_{0c}(\vec{R}_I, \vec{R}_J, E_j) \\ &\quad \times \langle \vec{R}_J, c | V | \vec{R}_J, c \rangle \langle \vec{R}_J, c | j \rangle. \end{aligned} \quad (2)$$

In this method, the potential matrix elements are derived from fitting particular experimental data. The physical content in the theory considered is tested by checking its predictions against independent data, and by requiring that the theory be internally consistent.

In what follows, we shall assume that the symmetry group of the impurity potential is at least a subgroup of that of the pure crystal (i.e.,  $T_d$  for zinc blende). If we label  $\vec{R}_I$  by its position,  $n$ , in the shell  $s$  of equivalent sites surrounding the impurity,<sup>23</sup> we can define a complete set of basis states<sup>23</sup>  $|LMNs\rangle$  for shell  $s$  consisting of orthonormal, linearly independent linear combinations of the Wannier states  $|sn\rangle$  which transform according to the  $M$  row of the  $L$  irreducible representation of the subgroup (we suppress the band index). The  $L$  involved are determined by decomposing the reducible representation derived by applying the subgroup operations to all the sites in a shell<sup>23, 35</sup> into the subgroup irreducible representations<sup>35</sup> (the presence of the index  $N$  allows for the possi-

bility of the same subgroup irreducible representation occurring more than once).

Since the same decomposition process can be performed with respect to  $T_d$ ,<sup>23</sup> and since the irreducible representations of a group are fully reducible<sup>35</sup> with respect to those of a subgroup, under the operations of the subgroup it is always possible to perform a similarity transformation such that all resulting basis function  $|LMN_K s\rangle$  of the same subgroup representation are among the basis functions of just the  $K$  irreducible representation of  $T_d$ .<sup>35</sup> In other words, if we decompose the  $K$  irreducible representation of  $T_d$  into the direct sum of the  $L_1, \dots, L_p$  irreducible representation of the subgroup, then the set of all these  $|L_i MN_K s\rangle$  ( $1 \leq i \leq p$ ) constitutes a basis for  $K$ . We let  $M$ , therefore, denote the corresponding row of the  $K$  representation. The value of this result is that these bases retain the symmetry properties of the representation of  $T_d$  from which they are derived. This notation preserves the label  $K$  of the corresponding representation of  $T_d$ .

That we are interested in luminescence properties simplifies the discussion considerably. The momentum amplitude of the impurity can be written

$$\langle \vec{k} | j \rangle = \sum_{LMN_K s} \langle \vec{k} | LMN_K s \rangle \langle LMN_K s | j \rangle, \quad (3a)$$

$$\begin{aligned} \langle \vec{k} | LMN_K s \rangle &= \sum_n \langle \vec{k} | sn \rangle \langle sn | LMN_K s \rangle \\ &= \frac{1}{(N_0)^{1/2}} \sum_n \exp(-i\vec{k} \cdot \vec{R}_{sn}) \\ &\quad \times \langle sn | LMN_K s \rangle, \end{aligned} \quad (3b)$$

$$\langle \vec{k} = 0 | LMN_K s \rangle = \frac{1}{(N_0)^{1/2}} \sum_n \langle sn | LMN_K s \rangle. \quad (3c)$$

In Eqs. (3), the conduction-band Bloch state of mo-

$$\langle LMN_K'' s'' | j \rangle = \sum_{N_Q s, N_K s'} \langle LMN_K'' s'' | G_0(E) | LMN_K' s' \rangle \langle LMN_K' s' | V | LMN_Q s \rangle \langle LMN_Q s | j \rangle. \quad (5a)$$

Since  $G_0$  is invariant under all operations of  $T_d$ , only states of the same row of identical irreducible representations of  $T_d$  enter in its matrix elements.<sup>35</sup> Matrix elements of  $G_0$  vanish between states corresponding to different  $\Gamma_1$  bases. Perhaps the simplest way to see this is to consider the trivial case  $V=C$ , a constant. For states of  $\Gamma_1$  symmetry, we have

$$\begin{aligned} \langle \Gamma_1 N_1 s | j \rangle &= C \sum_{N_1' s'} \langle \Gamma_1 N_1 s | G_0(E) | \Gamma_1 N_1' s' \rangle \\ &\quad \times \langle \Gamma_1 N_1' s' | j \rangle. \end{aligned} \quad (5b)$$

In deriving Eq. (5b), we have exploited the result that the  $|\Gamma_1 N_1 s\rangle$  are constructed to be orthonormal.

mentum  $\vec{k}$  is given by  $|\vec{k}\rangle$ , and the sums over  $n$  are over all sites in a shell [the transformation connection between Bloch and Wannier states is also given implicitly in Eq. (3b)].

For  $T_d$  and its subgroups, we can always<sup>35</sup> generate a completely symmetric function from the  $|sn\rangle$ ,<sup>23</sup> which transforms according to the trivial one-dimensional representation  $\Gamma_1$  (for which the representation matrix elements are unity for all the group elements and which we denote by  $K=1$ ),<sup>36</sup>

$$|\Gamma_1 1s\rangle \equiv |\Gamma_1 1_1 s\rangle \equiv \frac{1}{(n_s)^{1/2}} \sum_n |sn\rangle. \quad (4a)$$

The quantity  $n_s$  denotes the number of sites in shell  $s$ , the sum is over all sites within the shell, and the label  $N=1$  permits the possibility of other  $\Gamma_1$  representations for  $K=1$  in the shell decomposition. The basis vector orthogonality theorem<sup>35</sup> implies that<sup>37</sup>

$$\begin{aligned} \langle \Gamma_1 1s | LMN_K s \rangle &= 0 = \frac{1}{(n_s)^{1/2}} \sum_n \langle sn | LMN_K s \rangle \\ &\propto \langle \vec{k} = 0 | LMN_K s \rangle. \end{aligned} \quad (4b)$$

In Eq. (4b), the matrix element is taken with basis vectors from other, distinct representations (i.e.,  $K \neq 1$ ). If other  $\Gamma_1$  (i.e.,  $K=1$ ) representations exist in the decomposition, we can always construct them to be orthogonal to  $|\Gamma_1 1s\rangle$ .<sup>23</sup> Therefore,

$$\langle \vec{k} = 0 | j \rangle = \sum_s \left( \frac{n_s}{N_0} \right)^{1/2} \langle \Gamma_1 1s | j \rangle. \quad (4c)$$

To describe strong luminescence, therefore, we need to consider only those states which transform according to  $\Gamma_1$ . We should note that the energies of the states of other symmetries are not important in this discussion.<sup>38</sup>

The equation for the coefficients in Eq. (3a) which is analogous to Eq. (2) is

It is clear that the only change is a rigid shift in the bands by  $C$  and that  $|j\rangle$  corresponds to a Bloch state,  $|\vec{k}\rangle$ . Consider the state  $|\vec{k}=0\rangle$ . From Eqs. (3) and (4), we have

$$\begin{aligned} \langle \Gamma_1 N_1 s | \vec{k} = 0 \rangle &= \left( \frac{n_s}{N_0} \right)^{1/2} \delta_{N,1} \\ &= C \sum_{s'} \langle \Gamma_1 N_1 s | G_0(E) | \Gamma_1 1s' \rangle \left( \frac{n_{s'}}{N_0} \right)^{1/2}. \end{aligned} \quad (5c)$$

Since Eq. (5c) is true for all shells  $s$ , we see that it is consistent only if

$$\langle \Gamma_1 N_1 s | G_0(E) | \Gamma_1 1s' \rangle = \delta_{N,1} \langle \Gamma_1 1s | G_0(E) | \Gamma_1 1s' \rangle. \quad (5d)$$

The equation for the  $\langle \Gamma_1 1s | j \rangle$ , is therefore,

$$\begin{aligned} \langle \Gamma_1 1s | j \rangle = & \sum_{s', s'', N_K} \langle \Gamma_1 1s | G_0(E) | \Gamma_1 1s' \rangle \\ & \times \langle \Gamma_1 1s' | V | \Gamma_1 N_K s'' \rangle \\ & \times \langle \Gamma_1 N_K s'' | j \rangle. \end{aligned} \quad (6)$$

The derivation of Eq. (6) is independent of any specific model and is based upon symmetry arguments only. For an impurity potential whose symmetry is that of a subgroup of  $T_d$ , the  $\Gamma_1$  eigenstates are admixtures of the  $|\Gamma_1 N_K s\rangle$ , in general<sup>35</sup>; the number of states involved depends, of course, upon the compatibility relations between  $T_d$  and the subgroup and upon each shell decomposition. For example, for the first shell there is only one  $\Gamma_1$  which enters in the decomposition in terms of  $T_d$ .<sup>23</sup> As we lower the symmetry of the subgroup, more  $\Gamma_1$  can enter in the decomposition.<sup>39</sup>

At this point, we must use physical considerations in order to proceed further. If the matrix elements  $\langle \Gamma_1 1s | V | \Gamma_1 N_K s' \rangle$  in Eq. (6) are large, the admixture between the strongly luminescent  $|\Gamma_1 1s\rangle$  is strong. In this case, therefore, there can appear several lines of comparable strength. We should recall, however, that we set ourselves the problem of understanding in terms of an intermediate-range model the experimental observation that only the two lowest nitrogen lines in Fig. 1 are strongly luminescent (i.e., we ignore the strong  $N_\Gamma$  line in this study). The simplest procedure is to set  $\langle \Gamma_1 1s | V | \Gamma_1 N_K s' \rangle \sim \delta_{K,1} \delta_{N,1}$ : That is, the deviation of  $V$  from  $T_d$  symmetry is only a weak perturbation and the potential produces at least one state consisting of the  $|\Gamma_1 1s\rangle$  alone. This is a strong assumption, however. Even for potentials of  $T_d$  symmetry,  $\langle \Gamma_1 1s | V | \Gamma_1 N_1 s' \rangle$  does not vanish, in general: The matrix elements between Wannier functions depend upon the sites involved, in general.

Before considering the solutions for the nearest-neighbor shell model in detail, it is appropriate to discuss the matrix elements of the potential in Eq. (6). To accomplish this, let us treat two models corresponding to two opposite limits,

$$\langle sn | V_1 | s'n' \rangle = C \delta_{ss'}, \quad (7a)$$

$$\langle sn | V_2 | s'n' \rangle = V_s \delta_{nn'} \delta_{ss'}. \quad (7b)$$

The first of these corresponds to a potential whose Wannier-function matrix elements are independent of the distance between the sites at which these functions are centered: This would seem to be physically unrealistic. The second corresponds to a slowly varying potential which is the same for all sites in a shell (i.e., a "radial" dependence).

The matrix elements between basis states of two irreducible representations of the symmetry group of  $V$  derived from Eqs. (7) are given by

$$\begin{aligned} \langle LMN_K s | V_1 | L'M'N'_Q s' \rangle = & C \delta_{ss'} (n_s n_{s'})^{1/2} \\ & \times \langle LMN_K s | \Gamma_1 1s \rangle \\ & \times \langle \Gamma_1 1s' | L'M'N'_Q s' \rangle, \end{aligned} \quad (8a)$$

$$\langle LMN_K s | V_2 | L'M'N'_Q s' \rangle = V_s \delta_{ss'} \langle LMN_K s | L'M'N'_Q s' \rangle, \quad (8b)$$

$$\langle LMN_K s | LMN'_K s \rangle = \delta_{NN'}. \quad (8c)$$

If we restrict our attention to states arising from a single shell (e.g., the first<sup>23</sup>) we see that  $V_1$  will have nonvanishing matrix elements only between  $|\Gamma_1 1s\rangle$  states: States of other symmetries cannot exist. The potential  $V_2$ , on the other hand, produces identical matrix elements between any two states of the same row of the same irreducible representation [i.e., we construct different bases of the same representation to be orthogonal<sup>35</sup> so that Eq. (8c) applies]. It is clear, therefore, that only for the unrealistic potential  $V_1$  can we ignore states of other bases than  $|\Gamma_1 1s\rangle$  on the basis of matrix-element arguments.<sup>23</sup> In fact, these states are likely to be bound, as we see from considering  $V_2$ . It is only because these states are weakly luminescent that we can afford to ignore them.<sup>38</sup>

We are now in a position to examine the states arising from the nitrogen site and its nearest-neighbor shell. Using Eq. (6) and the fact that there is only one  $\Gamma_1$  state in the decomposition<sup>23</sup> of the nearest-neighbor shell representation, we derive equations of the same form as Eq. (E6) of Ref. 23 (although the interpretation of the potential matrix elements is somewhat different)

$$\begin{vmatrix} 1 + JG_{00} + b^*G_{01} & bG_{00} + LG_{01} \\ JG_{10} + b^*G_{11} & 1 + bG_{10} + LG_{11} \end{vmatrix} = 0, \quad (9a)$$

$$-J \equiv \langle \Gamma_1 10 | V | \Gamma_1 10 \rangle, \quad (9b)$$

$$-L \equiv \langle \Gamma_1 11 | V | \Gamma_1 11 \rangle, \quad (9c)$$

$$-b \equiv \langle \Gamma_1 10 | V | \Gamma_1 11 \rangle, \quad (9d)$$

$$G_{ss'} \equiv \langle \Gamma_1 1s | G_0(E) | \Gamma_1 1s' \rangle. \quad (9e)$$

The asterisk in Eq. (9a) denotes complex conjugation and  $s$  and  $s'$  are restricted to the values 0 and 1 in Eq. (9e).

Since this is a semiempirical model, we must extract the potential parameters from the two experimental energies  $E_{N\Gamma}$  and  $E_{N_K}$  in Fig. 1. Let us, for the time being, neglect the intersite matrix elements,  $b$ .<sup>23</sup> It is clear, therefore, that

$$(1 + JG_{00})(1 + LG_{11}) = JLG_{01}G_{10}, \quad (10)$$

must be satisfied for these two energies. This results in the following quadratic equation for  $L$ :

$$AL^2 + BL + C = 0, \quad (11a)$$

$$A \equiv G'_{11}D - G_{11}D', \quad (11b)$$

$$B \equiv G'_{11}G_{00} - G_{11}G'_{00} + D - D', \quad (11c)$$

$$C \equiv G_{00} - G'_{00}, \quad (11d)$$

$$D \equiv G_{00}G_{11} - G_{10}G_{01}. \quad (11e)$$

In Eqs. (11), the primed quantities are evaluated for  $E = E_{N_X}$  and the unprimed for  $E_{N_\Gamma}$ . There is, of course, a physically acceptable (i.e., real) solution for  $L$  if and only if

$$B^2 - 4AC = [(G'_{00} - G_{00})(G_{11} - G'_{11}) + G_{10}^2 + G_{10}'^2]^2 - 4(G_{10}G_{10}')^2 \geq 0. \quad (12a)$$

Here, we have employed the reality of the Green's function in the gap. The condition in Eq. (12a) is not satisfied (i.e., there is no real solution for  $L$ ) if

$$(G_{10} + G'_{10})^2 > (G_{00} - G'_{00})(G_{11} - G'_{11}) > (G_{10} - G'_{10})^2. \quad (12b)$$

In order to evaluate Eq. (12b), it is necessary to provide a calculation of the Green's functions defined in Eq. (9e). In the Appendix, we present a soluble model<sup>22</sup> of the Green's function based upon a parabolic  $E_c(\vec{k})$  for each minimum in the conduction band. The parameters of the model are adjusted to be consistent with our knowledge of the lowest conduction band. In contrast to other models<sup>3-8</sup> (as opposed to pseudopotential band-structure calculations<sup>23</sup>) this model can be readily applied to calculating  $G_{oc}(\vec{R}, \vec{R}')$  as well as  $G_{oc}(\vec{R}, \vec{R})$  [i.e., in the notation of Eq. (1)]: This would be useful in systematic comparison of N-N pair<sup>1</sup> and single-nitrogen states, for example. The results of the model are

$$G_{10} = \frac{1}{(12)^{1/2}} \sum_n G_{oc}(\vec{R}_{1n}, \vec{R}_0, E), \quad (13a)$$

$$G_{00} = G_{oc}(\vec{R}_0, \vec{R}_0, E), \quad (13b)$$

$$G_{11} = \frac{1}{12} \sum_{n,m} G_{oc}(\vec{R}_{1n}, \vec{R}_{1m}, E), \quad (13c)$$

$$G_{oc}(\vec{R}, 0, E) = \sum_{i,l} H_{il}(E, \vec{R}) e^{i\vec{k}_{il} \cdot \vec{R}}, \quad (13d)$$

$$H_{il}(E, \vec{R}) = F(p_i, m_i^*, E_i, R_{il}, g_i, E), \quad (13e)$$

$$m_i^* \equiv (m_{i\perp} m_{i\parallel}^2)^{1/3}, \quad (13f)$$

$$R_{il} \equiv R \left[ \frac{m_{i\parallel}}{m_i^*} + \frac{m_{i\perp} - m_{i\parallel}}{m_i^*} \left( \frac{\vec{K}_{il} \cdot \vec{R}}{K_{il} R} \right)^2 \right]^{1/2}. \quad (13g)$$

The energies considered are in the gap. The quantities to be calculated in the inequality in Eq. (12b) are defined<sup>23</sup> in Eqs. (13a)–(13c) in terms of the

Wannier representation Green's function of Eqs. (1), which depends upon the difference between lattice vectors only, i.e.,

$$G_{oc}(\vec{R}, \vec{R}', E) = G_{oc}(\vec{R} - \vec{R}', 0, E).$$

In Eqs. (13d) and (13e), this latter Green's function is expressed as a sum over inequivalent minima (i.e., index  $l$ ) associated with a particular symmetry point in the Brillouin zone (i.e., index  $i$ ). The sum is in terms of a negative-definite universal function  $F$  of the parameters associated with each minimum. This function, which involves the exponential integral function of complex argument, is discussed in the Appendix. The longitudinal ( $m_{i\perp}$ ) and transverse ( $m_{i\parallel}$ ) effective masses of a general minimum are expressed through the effective mass  $m_i^*$ , and an effective displacement  $R_{il}$ , which differs from  $R$  only because of the anisotropy. The energy of the  $i$  minimum is symbolized by  $E_i$  and the quantity  $p_i$  denotes a cutoff momentum whose magnitude is related to the number of states associated with the minimum. The possibility of simulating finite lifetimes of conduction-band states is embodied in the energy width parameter  $g$  in Eq. (13e).

In our calculations for Ga(As, P), we divide the Brillouin zone into three regions associated with the  $\Gamma$ ,  $X$ , and  $L$  minima,<sup>10,11</sup> respectively, as in previous work,<sup>4-7,12,23</sup>  $0 < Q_r < 0.125$ ,  $0.125 < Q_r < 0.50$ , and  $0.50 < Q_r$ , where  $\vec{Q} \equiv \vec{k}a/2\pi$ ,  $a$  is the lattice constant, and the subscript  $r$  denotes a Cartesian coordinate of the vector. This results in a value of  $p_i a = (6\pi^2 V_{iQ}/n_{\min})^{1/3}$ , where  $V_{iQ}$  denotes the volume in  $Q$  of the  $i$  region and  $n_{\min}$  the number of inequivalent minima of the  $i$  minimum: We derive  $p_\Gamma a = 0.974$ ,  $p_X a = 3.898$ , and  $p_L a = 2.443$  (in our calculations, we set  $a = 3.65 - 0.20x \text{ \AA}$ ). The corresponding values of the Ga(As, P)  $E_i$  are<sup>1,10-11</sup>  $E_\Gamma = 1.514 + 1.174x + 0.186x^2$ ,  $E_X = 1.977 + 0.144x + 0.211x^2$ , and  $E_L = 1.802 + 0.77x + 0.16x^2$ . In addition, our purposes here allow us to set  $g_i = 0$  (i.e., no finite lifetime processes).

Results for the three Green's functions in the inequality in Eq. (12b) are presented as functions of energy in Fig. 2 for  $x = 0.50$  and an assumed isotropic effective mass at  $X$  (i.e.,  $m_X^*/m_0 = 0.366$ , where  $m_0$  is the free-electron mass,  $m_i^*/m_0 = 0.068 + 0.052x$ ,  $m_{L\parallel}/m_0 = 0.15$ , and  $m_{L\perp}/m_0 = 1.184$ ).<sup>40</sup> We relegate discussion of the comparison between the results of this model and pseudopotential calculations<sup>23</sup> to the Appendix and concentrate here on our stated purpose of examining the inequality in Eq. (12b). For this purpose, it is sufficient to observe that  $|G_{10}|$  is considerably smaller than either  $|G_{00}|$  or  $|G_{11}|$  and varies more rapidly.

In Figs. 3(a) and 3(b) we present a pictorial expression of the inequality in Eq. (12b) correspond-

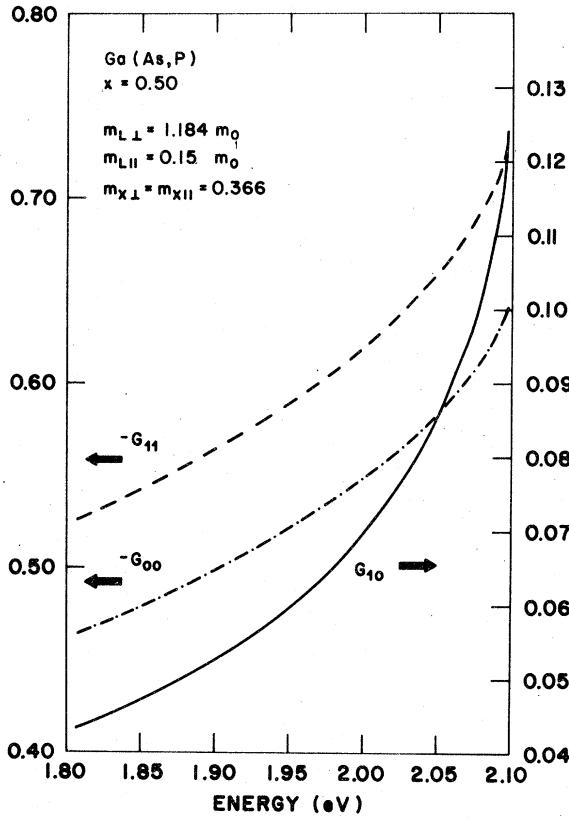


FIG. 2. Green's functions (in arbitrary units) defined in Eqs. (9) calculated from the soluble model in Eqs. (13) and the Appendix. The effective mass at X is assumed to be isotropic.

ing to the model in Figs. 2 (i.e., the same choice of masses) for  $x=0.35$  and  $0.50$ , respectively. The primed quantities  $G'_{00}$ ,  $G'_{11}$ , and  $G'_{10}$  are evaluated at the experimental energies  $E_{N_X}=1.857$  eV for  $x=0.35$  and  $1.944$  eV for  $x=0.50$  and the unprimed quantities are allowed to vary as functions of energy. Also depicted are the experimental energies of the higher state,  $E_N \equiv E_{N\Gamma} = 1.914$  eV for  $x=0.35$  and  $2.040$  eV for  $x=0.50$ . It is clear from Fig. 2 that, for  $0.30 < x < 0.50$ , the inequality in Eq. (12b) is satisfied, throughout the range of energies depicted so that there is no choice of parameters  $J$  and  $L$  which can fit the experimental energies, at least for this model Green's function. It should be noted that this result holds even though  $|G_{10}|$  is small. Mathematically, we obtain this result because we are examining essentially the *variation* of the Green's functions  $G_{00}$  and  $G_{11}$  (i.e., their relative values) and not their *absolute magnitudes*.

In order to illustrate the general validity of the inequality in Eq. (12b) for the Green's functions described in Eqs. (13), we display the Green's functions and the quantities involved in Eq. (12b)

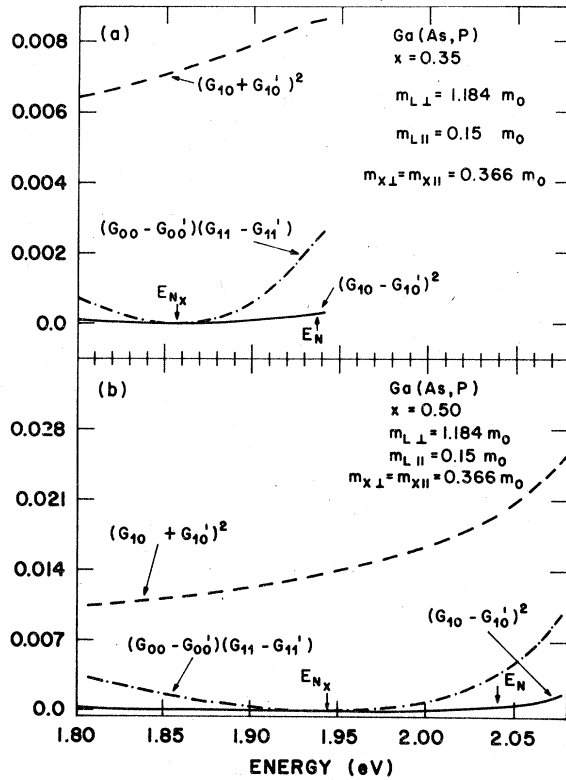


FIG. 3. (a) Test of the inequality in Eq. (12b) for  $x=0.35$  and the parameters of Fig. 1. (b) Test of Eq. (12b) for  $x=0.50$  and the parameters of Fig. 1. These figures demonstrate that the short range of the nearest-neighbor potential does not permit sufficient independence of the eigenstates in  $\vec{k}$  space to describe the data. The units are arbitrary.

for  $x=0.50$  in Figs. 4(a) and 4(b), respectively, for a set of anisotropic X masses<sup>10,11</sup> although  $m_X^*$  is the same as in Figs. 2 and 3; that is,  $m_{X\perp}/m_0 = 1.51$  and  $m_{X\parallel}/m_0 = 0.18$ ,<sup>40</sup> and all other parameters are the same as in Figs. 2 and 3. Although  $G_{00}$ , which depends upon  $m_i^*$  (i.e.,  $i=\Gamma, X, L$ ) only, is the same in Figs. 2 and 4(a), the  $\vec{R}$ -dependent Green's functions  $G_{11}$  and  $G_{10}$  are considerably different. In particular, the  $G_{10}$  in Figs. 2 and 4(a) are different not only in shape, but also in sign. This result derives from the summation over minima in Eq. (13d). The phases of the exponential factors depend upon the orientation of  $\vec{R}$  relative to the momentum positions of the minima. Also the  $F$  function in Eq. (13e) for each minimum depends not only upon this orientation but also upon the mass anisotropy through the  $R_{ii}$  in Eq. (13g). In general, the sign and magnitude of each term contributing to the Green's function through the sum in Eq. (13d) depends upon the orientation. The  $\vec{R}$ -dependent Green's function is, therefore, a sensitive function of anisotropy—the degree of

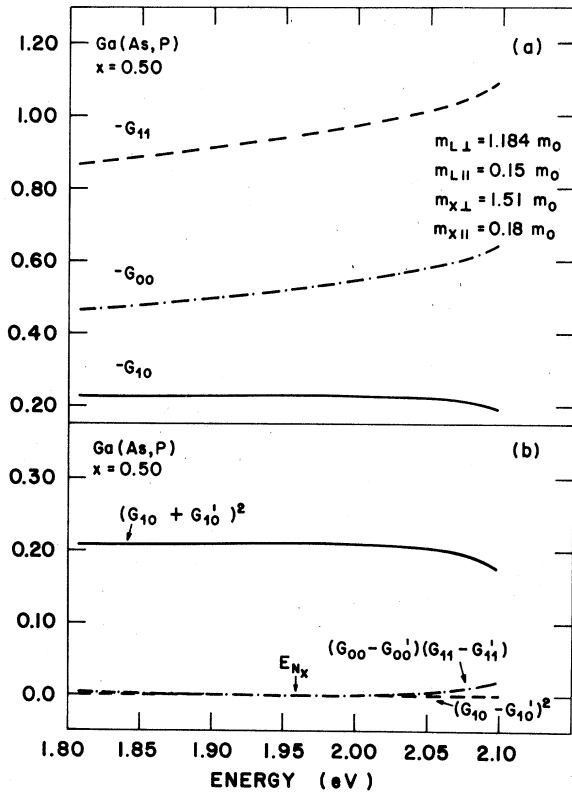


FIG. 4. (a) Green's functions defined in Eq. (9) for the model of Eq. (13) and the Appendix in arbitrary units. The  $X$  effective mass is anisotropic here and the other parameters are the same as in Fig. 1. This figure demonstrates the band-structure sensitivity of the Green's-function model. (b) Test of the inequality in Eq. (12b) for the Green's functions of Fig. 4(a). This figure illustrates the insensitivity of the inequality to the form of the Green's functions and emphasizes its fundamental relation to the range of the potential.

sensitivity can be appreciated by comparing Figs. 2 and 4(a).

The function  $G_{10}$  involves only nearest-neighbor lattice vectors [i.e.,  $NN_1$  separations<sup>1</sup>]. The contribution from the  $X$  minima is dominant because of the high density of states associated with this minimum. Of the phase factors of the three equivalent  $X$  minima in Eq. (13d), two contribute factors of  $-1$  and the third  $+1$ . In the case of isotropic  $X$  masses, the  $F$  of all the  $X$  minima are identical. The result for  $G_{0c}(R_{NN_1})$  involves, therefore,  $-F$ , which is positive definite, so that  $G_{10}$  in Fig. 2 is positive. In the case of anisotropic  $X$  masses, the  $F$  are orientation dependent. The two minima with negative phase factors involve [from Eq. (13g)]  $R_{Xl} = R(m_{Xl}/m_0)^{1/2} > R$ , and the positive phase factor minimum involves  $R_{Xl} = R(m_{Xl}/m_0)^{1/2} < R$ . The  $F$  function decreases with increasing  $R_{il}$  so that the positive-phase-factor term dominates in the sum in Eq. (13d) and  $G_{10}$  has

the same sign as  $F$ —negative, as in Fig. 4(a).

Similar arguments can be made to explain the behavior of  $G_{11}$  in Figs. 2 and 4(a). The situation is more complicated, however, because, from Eq. (13c),  $G_{11}$  involves all the lattice vectors separating sites in the first shell, and, therefore, many  $G_{0c}(\vec{R})$ . The difference between  $G_{11}$  in Fig. 2 and in Fig. 4(a), however, can be seen easily if we realize that  $G_{11}$  can be written as a sum of  $G_{00}$ ,  $G_{0c}(R_{NN_1})$  and other terms. Since, as we have just argued,  $G_{0c}(R_{NN_1})$  is negative for the parameters of Fig. 4(a) and positive for those of Fig. 2,  $G_{11}$  should be smaller (i.e., more negative) in the former case than in the latter. This is indeed illustrated in these figures.

The point of this technical discussion of the features of the Green's functions presented in Figs. 2–4 is that they are sensitive functions of the band structure (i.e., the mass anisotropy associated with the various minima). Even though the functions in Fig. 4(a) are probably a more accurate representation of the exact Green's functions than those in Fig. 2 (because the effective masses are more accurate<sup>40</sup>), the sensitivity suggests a considerable uncertainty in the final result. Nevertheless, the inequality in Eq. (12b) is satisfied in this case also, as manifested in Fig. 4(b). In fact, the inequality applies for all reasonable choices of effective mass throughout the experimental range  $0.30 < x < 0.50$  and the energy range under consideration (i.e., within  $\sim 0.200$  eV of the lowest conduction edge).

In Fig. 4(b), we display the quantities involved in the inequality in Eq. (12b) corresponding to the same parameters as Fig. 4(a). Here, we evaluate the primed Green's functions at the energy  $E_{N_X} = 1.954$  eV (i.e., we add 0.010 eV to account for bound excitons<sup>1</sup>). Because of the differences in the Green's functions in Figs. 4(a) and 2, which we have discussed, the energy dependences of the quantities in Fig. 4(b) are different from those in Fig. 3(b). It is clear, however, that Eq. (12b) is satisfied.

It would seem that these results could be an artifact of the model we have used. Fortunately, independent pseudopotential calculations of  $G_{00}$ ,  $G_{11}$  and  $G_{10}$  have been performed.<sup>23</sup> Application of these quantities to the inequality in Eq. (12b) yields the same result: *There are no parameters which allow Eq. (10) to describe the experimental energies.* We feel, in fact, that this conclusion reflects a fundamental mathematical and physical property of the data which is independent of any model. The analysis will enable us to extend these conclusions to the solution of Eq. (9a) (i.e., when arbitrary intershell matrix elements of the potential are included).

We begin by discussing the quantities involved in Eq. (12b) and Figs. 2-4. In general, we can expect  $|G_{10}|$  to be considerably smaller than  $|G_{00}|$ <sup>23</sup> because, from Eqs. (1c) and (13a),  $G_{10}$  involves interference between different conduction band states<sup>33</sup> contributing to the  $\vec{k}$  sum in Eq. (1c) (i.e.,  $G_{0c}(\vec{R}, 0, E)$  varies roughly as  $R^{-1}$  because of this).  $|G_{11}|$ , on the other hand, is expected to be of the same order as  $|G_{00}|$  because it can be expressed, from Eq. (13c), as a sum of  $G_{00}$  and  $\vec{R}$ -dependent terms. We can predict that

$$(G_{00} - G'_{00})(G_{11} - G'_{11}) > (G_{10} - G'_{10})^2$$

is satisfied. The question of whether potential parameters exist which solve Eq. (10) for two states of given energy rests, therefore, upon when

$$(G_{10} + G'_{10})^2 < (G_{00} - G'_{00})(G_{11} - G'_{11}).$$

The slower the variation in energy of  $G_{00}$  and  $G_{11}$ , the wider the range of energy for which Eq. (12b) is satisfied. For example, if  $G_{00} \sim G_{11} \sim G_{10} \sim 0$  (i.e., the energy is deep in the gap) we have  $G'_{10} < G'_{11} G'_{00}$  so that there are two solutions of Eq. (10) in this case. In fact, by inspecting Figs. 3 and 4(b), we observe that the upper and middle curves approach one another for large enough  $|E - E_{N_X}|$ .

More insight can be gained by examining the original equation, Eq. (10). Since  $G_{10} G_{01} \ll G_{00} G_{11}$ ,<sup>23</sup> it is tempting to ignore the right-hand side of Eq. (10) and write<sup>23</sup>

$$(1 + JG_{00})(1 + LG_{11}) = 0. \quad (14)$$

It is well known<sup>3-5, 12</sup> that even a small additional energy-dependent component can cause a large shift in the energy eigenvalue solutions of Eq. (14) because  $G_{00}$  and  $G_{11}$  are slowly varying.

The origin and meaning of this shift can be appreciated by considering an analogous equation, corresponding to a model for N-N pairs.<sup>1, 3</sup> In this model, we juxtapose two identical impurities at positions  $\vec{R} = 0$  and  $\vec{R} = \vec{R}_1$ . Each impurity is described by the same Koster-Slater parameter  $V_0$  which produces a state at energy  $E_0$  for an isolated impurity. The equation for the eigenvalues  $E_+$  and  $E_-$  resulting from the juxtaposition can be written in two equivalent forms, Eqs. (15a) and (15b),

$$\{1 - V_0[G(0, E_+) + G(R, E_+)]\} \times \{1 - V_0[G(0, E_-) - G(R, E_-)]\} = 0, \quad (15a)$$

$$[1 - V_0 G(0, E_{\pm})]^2 = [V_0 G(R, E_{\pm})]^2, \quad (15b)$$

$$1 - V_0 G(0, E_0) = 0, \quad (15c)$$

$$G(R, E) \equiv G_{0c}(\vec{R}, 0, E). \quad (15d)$$

These equations are expressed so that the analogy

with Eqs. (10) and (14) is obvious. Of the two eigenfunctions, one is bonding ( $E_+$ ) and one anti-bonding ( $E_-$ ), which is clear from Eq. (15a), and their energies are split. The magnitude of this splitting, depends upon  $V_0$ . The left-hand side of Eq. (15b) by itself produces eigenvalue  $E_0$ , so that it is the right-hand side which produces the splitting. Furthermore, from Eq. (15c), we see that  $V_0$  is uniquely determined by the Green's function at  $E = E_0$  (i.e., the band structure for all  $\vec{k}$ ). Therefore, the values of  $E_+$  and  $E_-$  are dependent only upon the band structure and  $E_0$ : In other words, there is a minimum energy splitting of the eigenvalues in the energy range of interest. This result reflects the general phenomenon<sup>35</sup> that two states of the same symmetry repel each other when coupled by a potential of the same (or higher) symmetry group. Here, we impose a condition on the potential through Eq. (15c)—this condition is implicit in a semiempirical treatment.

The same arguments apply to Eq. (10), although it is impossible to factor the equation as in Eq. (15a). The right-hand side of Eq. (10) produces splitting between the eigenvalues (i.e., they repel<sup>35</sup> each other). The magnitude of the splitting depends only upon the Green's function in the energy range of interest (i.e., it is a property of the band structure) and, therefore, has a minimum value. If we try, therefore, to determine the potential parameters  $J$  and  $L$  from energy eigenvalues (i.e., the experimental energies  $E_{N_X}$  and  $E_{N_\Gamma}$  in Fig. 1) whose separation is less than this minimum splitting, we find the task impossible—this is what the inequality in Eq. (12b) means. If we try to fit two energies whose separation is greater than this splitting, we find it possible. For example, an energy which is very deep in the gap could be fit by a solution associated with the central cell, and one which is shallow could be associated with the shell of nearest neighbors—but the energy separation must be big enough.<sup>23</sup>

What insight does this give us into the data? From this discussion, we know that the solutions of Eq. (10) are not independent—they are linked by a consistency relation which involves the band structure for *all*  $\vec{k}$  (i.e., *all* the conduction band minima). This reflects the basic nature of a potential whose range is limited. The experimental energies, on the other hand, are associated with independent conduction band minima. It is clear, therefore, that the data is not consistent with the intermediate-range potential we have considered as approximated by Eq. (10).

In a previous treatment,<sup>23</sup> similar data (whose similarity to that of Fig. 1 is within the uncertainties of our study) was fit to Eq. (14). Such a treatment neglects the fundamental points we have dis-

cussed.

In order to generalize our conclusions, we must take the intershell potential matrix element  $b$  into account. In this case, we derive, as in Ref. 23, for energies in the gap

$$(1 + JG_{00})(1 + LG_{11}) = JLG_{10}^2 + |b|^2(G_{00}G_{11} - G_{10}^2) - 2 \operatorname{Re}[b]G_{10}. \quad (16)$$

In Eq. (16) we explicitly show the reality of the  $G_{10}$  and denote the real part of  $b$  by  $\operatorname{Re}[b]$ .

The similarity between Eqs. (10) and (16), although striking, is hardly surprising. In view of our preceding discussion, we know that the first term on the right-hand side of Eq. (16) produced the splitting in our previous case. For  $J$  and  $L$  positive (i.e., attractive potentials), this term is positive: The more positive this term, the larger the splitting. Since  $G_{00}G_{11} > G_{10}^2$ , the second term is also positive in the gap. Finally, from the definition in Eq. (9d)

$$b = -\frac{1}{(12)V^2} \sum_n \langle 00 | V | 1n \rangle$$

where we use the  $|sn\rangle$  notation to describe Wannier states and the sum is over all the sites in the first shell. Consider one term in the sum

$$\operatorname{Re}[b_{0n}] = -\int d^3r V(\vec{r}) \operatorname{Re}[a_c^*(\vec{r}) a_c(\vec{r} - \vec{R}_{1n})], \quad (17)$$

where we denote the  $\vec{r}$ -space Wannier state  $\langle \vec{r} | sn \rangle$  by  $a_c(\vec{r} - \vec{R}_{sn})$  (i.e.,  $c$  denotes the conduction band). For negative potentials,  $V(\vec{r}) \leq 0$  for all  $\vec{r}$ . Therefore, the third term on the right-hand side of Eq. (16) is not independent of  $J$  and  $L$ . In order to fit the experimental energies,<sup>23</sup> it is necessary that  $J \sim L$ , so that  $V$  varies slowly in this region and  $b$  is small. From Figs. 3 and 4(b), we see that the inequality in Eq. (12a) is far from being satisfied. Therefore, inclusion of  $b$  for monotonic negative potentials does not improve matters. *We conclude that the data in Ga(As,P):N do not arise from an attractive potential which is always negative whose range is restricted to the nitrogen site and the first shell of nearest neighbors.*

This conclusion is quite strong and general. But under what conditions can it be violated, i.e., under what conditions do our arguments break down so that it might be possible to find solutions of Eq. (16) for the experimental energies? One obvious possibility is that the sum of the second and third terms on the right-hand side of Eq. (16) is negative. In this case, we must have

$$0 < |b| < 2[(\operatorname{Re}[b])/|b|] [G_{10}/(G_{00}G_{11} - G_{10}^2)] \\ \leq 2|G_{10}|/(G_{00}G_{11} - G_{10}^2).$$

Consider first  $J$  and  $L$  positive (i.e., attractive).

From the mathematical form of Eq. (16), in order to have two solutions within the energy range of interest, it is necessary to have values of  $J$  and  $L$  approximately equal to those which give eigenvalues within this range in Eq. (14); these values of  $J$  and  $L$  are approximately constant throughout this range because a small change in these parameters produces large shifts in the energy eigenvalues.<sup>5,12</sup> Such values of  $J$  and  $L$  have been determined<sup>23</sup> to be  $J = -0.6796 + 0.1126x$  and  $L = -0.7959 + 0.5371x$  in units of eV and, therefore  $J$  and  $L$  are of the same order for  $0.30 < x < 0.50$ .

Consequently, the potential must be negative and of the same order of magnitude in the regions of both the central cell and the first shell of nearest neighbors [i.e., see Eqs. (8) for limiting cases of the potential matrix elements and Eqs. (9) for the definitions of  $J$ ,  $L$ , and  $b$ ]. A value of  $\operatorname{Re}b < 0$  corresponds, therefore, to a region between the central cell and the first shell where  $V$  is positive. Physically, this positive barrier assists in localizing the eigenfunctions in regions of the central cell and first shell, respectively—that is, it helps to make the impurity states more independent of each other.

There are some problems with applying this type of potential to a model in which the range of the potential is restricted to the first shell of nearest neighbors. First, this potential is negative at the origin and in the first shell, and is positive in between, i.e., it is oscillatory and, because the amplitudes of these oscillations are of the same order of magnitude, it decays slowly. There is little physical reason, therefore, to suppose that the range of this potential is restricted to the first shell. Another problem is that such an oscillatory potential is very difficult to explain physically.

It should be emphasized that the potentials which we have just discussed only represent the situations where our proof of the inconsistency of this model and the Ga(As,P):N data breaks down. This by no means suggests that the model is consistent with the data in these cases—such consistency should be investigated through calculations.

We have, therefore, shown that, except possibly for rather pathological potentials, *the experimental energies in Ga(As,P):N cannot arise from the nearest-neighbor shell model.*<sup>23</sup>

## B. Ranges beyond the nearest-neighbor shell

In the last section, we showed that the experimental nitrogen lines in Ga(As,P):N cannot arise from an attractive, nondecreasing potential centered at the impurity site whose range does not extend beyond the shell of nearest-neighbor cells. In this, we argue that such a potential producing

these lines cannot have a range less than that of a square-well potential to which the effective-mass approximation is applicable (i.e., a range  $\sim 20\text{--}25 \text{ \AA}$ ).<sup>19,22</sup>

The logical sequence begins with the argument that, of all nondecreasing, attractive potentials of the same range, symmetry and ground-state energy, a constant potential (i.e., a "square well" which is not necessarily spherically symmetric) produces the first excited bound state of lowest energy (i.e., highest binding energy). Next, we show that, of two square-well potentials with the same ground-state symmetry and energy, the one with longer range produces the lower excited state. From this, we reason that, if we can identify the experimental energies  $E_{N_X}$  and  $E_{N_\Gamma}$  with bound states of a square-well impurity potential whose range is long enough for the effective-mass approximation to be valid,<sup>19,22</sup> then there is no intermediate-range potential of shorter range which can fit these energies. We complete the discussion by referring to the fact that the experimental data has been described by a square-well potential with a range of  $20\text{--}25 \text{ \AA}$ ,<sup>19,22</sup> so that no potential of shorter range can produce the experimental lines.

The argument rests upon the assumption that an excited state of a given symmetry is less localized at the "origin" (i.e., the impurity site) than is a state of the same symmetry of lower energies (i.e., higher binding energy). Also, we assume that the experimental energies can be identified with the nondegenerate ground and an excited state of an impurity potential which couples only to the lowest conduction band, as in Eq. (2).

Consider an attractive (i.e., negative) nondecreasing impurity potential  $V'$  of finite range whose eigenstates obey the following equation:

$$(H_0 + V')|\Psi'_i\rangle = E'_i|\Psi'_i\rangle, \quad (18a)$$

where  $H_0$  denotes the Hamiltonian of the perfect crystal and  $|\Psi'_0\rangle$  and  $|\Psi'_1\rangle$  correspond, respectively, to the ground state and a nondegenerate excited bound state of the impurity potential.

We can always define a constant potential  $V$  which is nonzero in exactly the same region as  $V'$  and zero elsewhere. Along every equipotential surface of  $V'$ ,  $V$  is also constant, so that the two potential energies have the same symmetry. The corresponding Schrödinger equation is

$$(H_0 + V)|\Psi_i\rangle = E_i|\Psi_i\rangle, \quad (18b)$$

where  $|\Psi_0\rangle$  denotes the ground state.

The point here is to show that, if we identify  $E'_0$  with  $E_{N_X}$ , then  $E'_1 - E'_0$  decreases monotonically with increasing range until  $E'_1 = E_{N_\Gamma}$  if the range is sufficiently long. We adjust  $V$ , therefore, until

$E_0 = E'_0$ . Because  $V$  and  $V'$  are assumed to couple only to the lowest conduction band, the  $|\Psi_i\rangle$  and  $|\Psi'_i\rangle$  are derived solely from conduction-band states and form complete sets with respect to these band states. We can, therefore, apply the variational principle to derive

$$E_0 \leq \langle \Psi'_0 | H_0 + V | \Psi'_0 \rangle = E'_0 + \langle \Psi'_0 | V - V' | \Psi'_0 \rangle, \quad (19a)$$

$$\langle \Psi_0 | V - V' | \Psi_0 \rangle \leq E_0 - E'_0 \leq \langle \Psi'_0 | V - V' | \Psi'_0 \rangle. \quad (19b)$$

Since  $E_0 - E'_0 = 0$ , the inequalities are not satisfied if  $V' \geq V$  for all  $\vec{r}$ . There must exist some equipotential surface along which  $V' = V$ . This surface separates the range of the potential into two regions. In the one closer to the impurity site, which we denote as region I,  $V - V' \geq 0$  because of the nondecreasing nature of  $V'$ . In the exterior region, or region II, we have  $V - V' \leq 0$ . Because  $\langle \Psi'_0 | V - V' | \Psi'_0 \rangle \geq 0$ ,  $\Psi'_0(\vec{r}) \equiv \langle \vec{r} | \Psi'_0 \rangle$  must be more concentrated in region I; on the other hand  $\Psi_0(\vec{r})$  must be more localized in region II. This is physically reasonable since a square well state must be less localized near the origin than the corresponding state of a more localized potential.

The difference in energies between  $E_0$  and  $E'_0$  is given by

$$\begin{aligned} (E_0 - E'_0) \langle \Psi_0 | \Psi'_0 \rangle &= \langle \Psi_0 | H_0 + V - (H_0 + V') | \Psi'_0 \rangle \\ &= \langle \Psi_0 | V - V' | \Psi'_0 \rangle = 0. \end{aligned} \quad (19c)$$

In Eq. (19c), we see that the larger concentration of  $\Psi'_0(\vec{r})$  in region I is exactly balanced by the localization of  $\Psi_0(\vec{r})$  in region II. Or, to put it another way, if we fix  $V$  and vary  $V'$  keeping  $E'_0$  fixed, the smaller the value of  $V - V'$  (that is, the less deep  $V'$ ) in region II, the more localized  $\Psi'_0(\vec{r})$  in region I.

Now, since  $E'_1 > E'_0$ , the wave function  $\Psi'_1(\vec{r})$  is more spread out than is  $\Psi'_0(\vec{r})$ . This property can, of course, be considered a reflection of orthogonality and implies a lower proportion of  $|\Psi'_1(\vec{r})|^2$  in the region where  $|\Psi'_0(\vec{r})|^2$  is large (i.e., the region of deep potential, near the impurity site) than in region II. We make, therefore, the physically reasonable assumption that

$$\langle \Psi'_0 | V - V' | \Psi'_0 \rangle_I \geq \langle \Psi'_1 | V - V' | \Psi'_1 \rangle_I \geq 0, \quad (20a)$$

$$\langle \Psi'_1 | V' - V | \Psi'_1 \rangle_{II} \geq \langle \Psi'_0 | V' - V | \Psi'_0 \rangle_{II} \geq 0, \quad (20b)$$

where the subscripts I and II denote integration over the corresponding regions. Equations (20) presume that the states are concentrated mostly within the range of the potential.

As a consequence of these physically reasonable assumptions, we have

$$\langle \Psi'_1 | V' - V | \Psi'_1 \rangle \geq \langle \Psi'_0 | V' - V | \Psi'_0 \rangle. \quad (20c)$$

The reasoning leading to Eq. (20c) is independent of our specific choice of  $V$  and  $V'$  and only requires that we can divide  $V' - V$  into two regions, in one of which (i.e., region I, in our case)  $V' - V \leq 0$ , and in the other (i.e., region II)  $V' - V \geq 0$ . Henceforth, we assume the validity of Eq. (20c) for any pair of such potentials.

For an impurity potential in a crystal, these statements make sense within the context of the Wannier representation, as in either Eq. (2) or its differential analog.<sup>24</sup> We have

$$[E_c(-i\hbar\nabla) - E]\langle\vec{R}|\Psi\rangle + \sum_{\vec{R}'}\langle\vec{R}|V|\vec{R}'\rangle\langle\vec{R}'|\Psi\rangle = 0, \quad (21)$$

where the derivative is evaluated at lattice site  $\vec{R}$ . The assumptions we have made, however, are general and motivated by fundamental quantum mechanical considerations.<sup>41</sup>

Consider a potential energy

$$V_g \equiv V + g(V' - V), \quad (22a)$$

where  $g$  is a coupling constant,  $0 < g < 1$ . This potential is intermediate between  $V$  and  $V'$  (i.e.,  $V_0 = V$  and  $V_1 = V'$ ). Define normalized eigenstates  $|\Phi_i(g)\rangle$  such that

$$(H_0 + V_g)|\Phi_i(g)\rangle = W_i(g)|\Phi_i(g)\rangle, \quad (22b)$$

$$|\Phi_1(1)\rangle \equiv |\Psi'_1\rangle, \quad W_1(1) \equiv E'_1, \quad (22c)$$

$$|\Phi_0(1)\rangle \equiv |\Psi'_0\rangle, \quad W_0(1) \equiv E'_0. \quad (22d)$$

Therefore,  $|\Phi_1(1)\rangle$  and  $|\Phi_1(0)\rangle$  are derived from the same one-dimensional irreducible representation of the symmetry group of the potential as  $|\Psi'_1\rangle$  (i.e.,  $V$ ,  $V'$ , and  $V_g$  have the same symmetry).

For  $g=0$ , we define

$$|\Psi_1\rangle \equiv |\Phi_1(0)\rangle, \quad E_1 \equiv W_1(0). \quad (22e)$$

The point is that if we can identify the experimental energies with two nondegenerate states  $E'_0$  and  $E'_1$  of an assumed potential  $V'$  then we can always make the correspondence in Eqs. (22). This does not guarantee that  $|\Psi_1\rangle$  will be bound; if, however, we can show that  $E_1 \leq E'_1$ , then the correspondence is well defined since  $|\Psi_1\rangle$  will be bound.

From an elementary theorem,<sup>42</sup> we know that, since  $\langle\Phi_i(g)|\Phi_i(g)\rangle = 1$ ,

$$\frac{d}{dg}W_i(g) = \langle\Phi_i(g)|V' - V|\Phi_i(g)\rangle, \quad (23a)$$

$$W_1(1) - W_1(0) = E'_1 - E_1 = \int_0^1 dg \langle\Phi_1(g)|V' - V|\Phi_1(g)\rangle, \quad (23b)$$

$$W_0(1) - W_0(0) = E'_0 - W_0(0) = \int_0^1 dg \langle\Phi_0(g)|V' - V|\Phi_0(g)\rangle. \quad (23c)$$

We have refrained from discussing the evolution of  $|\Phi_0(g)\rangle$  as  $g$  approaches zero. If, however, the ground states  $|\Psi_0\rangle$  and  $|\Psi'_0\rangle$  are derived from the same one-dimensional irreducible representation of the symmetry group of the potential, then  $|\Phi_0(0)\rangle = |\Psi_0\rangle$ . This is reasonable since these are nondegenerate eigenstates corresponding to the same symmetry group. We can, therefore, identify  $|\Phi_0(g)\rangle$  with the ground state of  $H_0 + V_g$ . From Eq. (22a), in region I,  $V_g \leq V$ . On the dividing surface between regions I and II,  $V_g = V$ . Therefore, the potential  $V_g$  satisfies the conditions leading to Eq. (20c), so that we can write

$$\langle\Phi_1(g)|V_g - V|\Phi_1(g)\rangle \geq \langle\Phi_0(g)|V_g - V|\Phi_0(g)\rangle, \quad (24a)$$

$$V_g - V = g(V' - V). \quad (24b)$$

Applying Eqs. (24) to Eqs. (23), we have

$$E'_1 - E_1 \geq \int_0^1 dg \langle\Phi_0(g)|V' - V|\Phi_0(g)\rangle = E'_0 - W_0(0). \quad (25a)$$

Therefore, under the condition that the ground states of  $V$  and  $V'$  can be derived from one another through Eqs. (22) and (23) (i.e., they have the same symmetry), we have

$$E'_1 - E_1 \geq E'_0 - E_0 = 0. \quad (25b)$$

In applying these results to the physical situation obtaining in  $\text{Ga(As, P):N}$ , we have few restrictions. Suppose that we can associate  $N_X$  and  $N_\Gamma$  with the ground and an excited state, respectively, of a given symmetry (i.e.,  $\Gamma_1$  symmetry, as discussed in Sec. IIA) produced by a specific nondecreasing potential,  $V'$ . In order to study the evolution of the states as a function of range, we construct all nondecreasing potentials  $V$  of longer finite range which have ground states of the same symmetry and whose ground-state energies are equal to  $E_{N_X}$ . By the same argument which allowed us to divide the range in which  $V' - V \neq 0$  into a positive region (i.e., region II) and a negative region (i.e., region I) for a  $V$  which is constant, we can make the same division for a  $V$  which varies (but does not decrease) and which has longer range (we consider this a definition of  $V$ ). From Eq. (25b), we see that the excited state energies for these longer-range potentials decrease with increasing range (i.e., the longer the range, the more states which are bound<sup>41</sup>).

From previous work,<sup>19,22</sup> we know that the experimental energies can be described by a spherical square-well potential for which the effective-

mass approximation is applicable (i.e., the range  $\sim 20\text{--}25 \text{ \AA}$ ). In particular,  $N_X$  corresponds to the nondegenerate ground state of  $\Gamma_1$  symmetry which is associated with  $X$  and  $N_\Gamma$  corresponds to a nondegenerate excited state bound to  $\Gamma$  [i.e., the lowest ( $\Gamma_1$ ) effective-mass state associated with  $\Gamma$ ]. Any other nondecreasing potential (whose ground-state energy is equal) of the same (long) range must have a corresponding excited state of *higher* energy, from Eq. (25b). These remarks are independent of symmetry since the square-well states are nondegenerate and will not be split if we add a small (e.g., vanishing) potential of lower symmetry. Obviously, any potential of shorter range whose ground state has the same symmetry and energy  $E_{N_X}$  has a yet higher excited state. Therefore, the range of  $20\text{--}25 \text{ \AA}$  should be thought of as a *lower* limit.

In deriving these results, we assumed that the ground state of the intermediate-range potential  $V'$  can be derived from that the "stronger" potential  $V$  (i.e., either a square-well or longer-range potential) in the sense of Eqs. (22) and (23). If Eq. (20c) is valid, then the states of  $V$  must keep the same order in energy as those of  $V'$  from which they are derived [i.e., the derivative in Eq. (23a) is always greater for the excited state than for the ground state, so the excited-state energy must rise more sharply and fall less steeply than that of the ground-state as we change  $g$  from zero to unity]. It should be emphasized that the criterion for the  $V$  which we select is that Eq. (20c) be obeyed, i.e., that most of the probability for the excited state be within the range of the potential—and this is always possible. Therefore for  $\Gamma_1$  ground states of  $V'$ , Eq. (25b) seems to be valid.

The above reasoning fails if the ground state of the intermediate range potential is not of  $\Gamma_1$  symmetry. But, then, by Eq. (4b), this state cannot account for  $N_X$ .

### III. CONCLUSIONS

Two of the experimentally measured nitrogen-line energies in Ga(As, P):N (i.e.,  $E_{N_X}$  and  $E_{N_\Gamma}$  in Fig. 1<sup>20,21</sup>) seem to be associated with the independent conduction-band minima  $X$  and  $\Gamma$ , respectively.<sup>14-16, 19, 20, 23, 27</sup> These have been explained theoretically in terms of states arising from a long-range nitrogen potential<sup>19,22</sup> and states produced by an intermediate range nitrogen potential.<sup>23</sup> The possibility of such a strain-induced long-range potential implies important consequences for studies of impurity-induced lattice relaxation in semiconductors. It is fundamentally important to understand the extent to which the nitrogen data is consistent with intermediate-range, as

opposed to long-range (i.e.,  $20\text{--}25 \text{ \AA}$ ), potentials. Our basic conclusion is that it is not, except, perhaps, for potentials which are difficult to justify physically.

In Sec. IIA, we make as general an examination as we can of a generalized version of a model introduced earlier,<sup>23</sup> an attractive potential limited to the nitrogen site and the first shell of nearest-neighbor cells. We find that such a model cannot describe the measured energies. The basic reason is that the eigenstates are delocalized in  $\vec{k}$  space and, therefore, involve both the  $\Gamma$  and  $X$  minima. They cannot be independent unless their energy separation is sufficiently large so that, in  $\vec{r}$  space, the deeper state is localized near the impurity and the more shallow state is concentrated in the shell [i.e., in  $\vec{k}$  space, the deeper eigenstate is relatively flat and the shallower is peaked near the conduction-band minima—a result of the characteristic  $[E - E_c(\vec{k})]^{-1}$  dependence]. For the band structure of Ga(As, P), we find that the experimental energies do not fulfill the energy-separation criterion and, therefore, cannot be described by independent eigenstates of this model. To derive this result we introduce a new, soluble model (which we describe in the Appendix) of the Wannier-space Green's function of Eq. (1c) (i.e., the result also holds true when we use a Green's function derived from pseudopotential band calculations<sup>23</sup>).

When we include physically reasonable nonzero intershell matrix elements, we find that the two eigenstates are again coupled, so that the above conclusions of inconsistency apply also in this case.

The nearest-neighbor shell model can be thought of as a longer range version of the single-site Koster-Slater model,<sup>3-9,13</sup> which we can think of as producing at most one bound ground-state and an excited state of infinitely high energy. As we transform the latter model into the former by adding a shell, we move the excited state down to a finite energy.

As we increase the range still further by adding yet more shells (always keeping the ground state energy equal to  $E_{N_X}$ ) does the excited move down still further? In Sec. IIB, we answer this question affirmatively. If we can vary the potential smoothly so that we transform the ground state into that corresponding to the longer range potential (both with the same energy), then the excited state has a lower energy in the longer-range case. This result is intuitively obvious, but we present a rather general proof here. One of the consequences is that a square-well potential has the minimum range of all nondecreasing attractive potentials which produce two such states of fixed energy.

Since we eventually reach the domain where the

effective mass approximation is valid by adding enough shells, we see that if the energy difference is still too large in this long range case, then it *never* agrees with experiment for a shorter range. Since the data can be fit<sup>19,22,26</sup> to a square-well potential of range 20–25 Å, we see that this value should be thought of as a *lower* limit.<sup>43-45</sup>

The reasoning presented here breaks down if the potential has *two* minima (e.g., one at the impurity site and one in the first shell). This type of oscillatory potential is hard to justify physically if one assumes that it arises from the impurity (so that it should decrease more or less monotonically with increasing distance from the nitrogen). If such a potential exists, however, it supports our contention that the impurity induces large relaxation of the lattice.

Another possibility is that such an oscillatory potential is produced by effects not associated with nitrogen (e.g., such as disorder) and that the impurity has favorable binding energy to enter such a region. The short range core<sup>1</sup> would then allow excited states to be observed<sup>19,22</sup> because of the high ( $\bar{k}=0$ ) recombination probability. Since such states have *not* been seen with other impurities, we discard this possibility.

#### ACKNOWLEDGMENTS

We would like to thank A. Kiel for helpful discussions on group theory. This work was supported in part by FAPESP, CNPq, and FINEP of Brazil.

#### APPENDIX: SOLUBLE MODEL OF THE CRYSTAL GREEN'S FUNCTION

Here we describe the model used in Sec. II A and Figs. 2–4 for the Green's function in the Wannier representation [i.e., Eq. (1c)] for the lowest conduction band,

$$G_{oc}(\vec{R}, 0, E) = \frac{\Omega}{(2\pi)^3} \int_{BZ} d^3k \frac{e^{i\vec{k}\cdot\vec{R}}}{E - E_c(\vec{k}) + ig}, \quad (A1)$$

where  $\Omega = \frac{1}{4}a^3$  is the volume of a unit cell, and the subscript BZ denotes integration over the first Brillouin zone.

We model each inequivalent minimum by a parabolic dispersion relation,

$$E_c(\vec{k}) = E_j + \hbar^2 \left( \frac{q_\perp^2}{m_{j\perp}} + \frac{q_\parallel^2}{m_{j\parallel}} \right), \quad (A2a)$$

$$E_j \equiv E_c(\vec{K}_{j1}), \quad (A2b)$$

$$q_\perp \equiv (\vec{k} - \vec{K}_{j1}) \cdot \vec{K}_{j1} / K_{j1}, \quad (A2c)$$

$$q_\parallel \equiv |\vec{k} - \vec{K}_{j1} - (\vec{K}_{j1} / K_{j1}) q_\perp|. \quad (A2d)$$

The symbols  $\perp$  and  $\parallel$  denote longitudinal and trans-

verse components, respectively (note that this convention is the reverse of that usually used), and  $\vec{K}_{j1}$  represents the  $\vec{k}$  position of the  $l$  inequivalent minimum of the  $j$  type (e.g., there are three minima at  $X$ ). The quantity  $g$  represents an energy width  $0^+$  in the pure crystal.

We can, therefore, express  $G_{oc}$  as a sum of contributions from each minimum,

$$G_{oc}(\vec{R}, 0, E) = \sum_{j,l} H_{jl}(E, \vec{R}) e^{i\vec{K}_{j1} \cdot \vec{R}}, \quad (A3a)$$

$$H_{jl}(E, \vec{R}) \equiv F(p_j, m_j^*, E_j, R_{j1}, g_j, E), \quad (A3b)$$

$$F(P, m, W, R, g, E)$$

$$\equiv \frac{\Omega}{(2\pi)^2} \int_0^P dp p^2 \int_{-1}^1 dx \frac{e^{ipR}}{E - W - \hbar^2 p^2 / 2m + ig} \\ = - \left( \frac{\Omega m}{(\hbar\pi)^2 R} \right) I, \quad (A3c)$$

$$I \equiv \frac{1}{4} i \{ e^{it} [E_1(it_-) - E_1(it_+) - 2\pi i] \\ + e^{-it} [E_1(-it_+) - E_1(-it_-)] \}, \quad (A3d)$$

$$t_\pm \equiv t \pm PR, \quad (A3e)$$

$$t \equiv \left( \frac{2m}{\hbar^2} \right)^{1/2} R [(E - W) + ig]^{1/2}, \quad (A3f)$$

$$R_{j1} \equiv R \left[ \frac{m_{j\parallel}}{m_j^*} + \frac{m_{j\perp} - m_{j\parallel}}{m_j^*} \left( \frac{\vec{K}_{j1} \cdot \vec{R}}{K_{j1} R} \right)^2 \right]^{1/2}, \quad (A3g)$$

$$m_j^* \equiv (m_{j\perp} m_{j\parallel}^2)^{1/3}. \quad (A3h)$$

In Eq. (A3c), we display explicitly that we have transformed from  $\vec{k}$  space where the energy is ellipsoidal, to  $\vec{p}$  space, where it is spherical. In this transformation, the vector  $\vec{R}$  is changed into  $\vec{R}_{j1}$ , whose magnitude is given in Eqs. (13g) and (A3g). The definition of the  $\vec{p}$  vector [i.e.,  $\vec{p}_\perp \equiv \vec{k}_\perp (m_j^* / m_\perp)^{1/2}$  and  $\vec{p}_\parallel \equiv \vec{k}_\parallel (m_j^* / m_\parallel)^{1/2}$ ] involves the masses, which accounts for the appearance of  $m_j^*$ , which is defined in Eqs. (13f) and (A3h).

The function  $E_1$  appearing in Eq. (A3d) is the exponential integral of complex argument

$$E_1(Z) \equiv \int_Z^\infty \frac{e^{-u}}{u} du \quad (A4)$$

where  $Z$  is a complex number.

The quantity  $p_j$  is defined by the requirement that the volume in  $\vec{k}$  space contain the number of states,  $N_j$ , associated with the  $j$  point, so that, if  $g=0^+$  (as in all our calculations),

$$p_j = 1/a(24\pi^2 N_j / n_{\min})^{1/3}, \quad (A5)$$

where  $n_{\min}$  symbolizes the number of inequivalent minima associated with  $j$ .

Finally, the presence of the quantity  $g_j$  in Eq. (A3b) allows the possibility of phenomenologically

accounting for scattering processes which limit the lifetimes of states in the  $j$  minimum. Notice that if  $g_j \neq 0$ ,  $\text{Im}[G_{0c}] \neq 0$  in the gap (where  $\text{Im}$  represents the imaginary part) in contrast to the case when

$$g_j = 0^+.$$

For usefulness in possibly applying this model to other situations we present some simple limiting cases,<sup>12,22</sup>

$$\text{Im}[F(P, m, E_j, R, 0, E)] = -\frac{\Omega m}{2\pi R \hbar^2} \sin(s_j R) \Theta(E - E_j), \quad (\text{A6a})$$

$$\text{Im}[F(P, m, E_j, 0, 0, E)] = -\frac{\Omega m}{2\pi \hbar^2} s_j \Theta(E - E_j), \quad (\text{A6b})$$

$$F(P, m, E_j, 0, g, E) = -\frac{\Omega m}{(\hbar\pi)^2 R} \left\{ PR + \frac{1}{2} t_j \left[ \ln \left( \frac{PR - t_j}{PR + t_j} \right) + i\pi \right] \right\}, \quad (\text{A6c})$$

$$s_j \equiv (2m/\hbar^2)(E - E_j), \quad t_j \equiv R(s_j^2 + 2img/\hbar^2)^{1/2}. \quad (\text{A6d})$$

Previous soluble models applied to this problem<sup>3-9</sup> either readily supplied  $G_{0c}$  for  $R=0$ , but not for finite  $R$  or calculated  $G_{0c}$  for  $R \neq 0$  from a free-space Green's function<sup>3</sup> so that the  $R=0$  value diverged because of the infinite  $\vec{k}$ -space volume in Eq. (A1). We present the first soluble model in which the  $R=0$  and  $R \neq 0$  values of  $G_{0c}$  are consistently derivable from one another.

The results of pseudopotential band-structure calculations were used to calculate  $G_{0c}$  for Ga(As, P).<sup>23</sup> These calculations are expected to represent the total conduction-band density of states much more accurately than in the simple parabolic model of Eqs. (A2) and (A3). The latter, however, employs the experimentally determined effective masses and energy positions of the minima. It should, therefore, be rather accurate close to the edge of a minimum.

Deep in the gap, the Green's function is insensitive to the details of the density of states. Near the edge, its structure (e.g., the discontinuity in the derivative<sup>3</sup>) is determined by the band structure near the bottom of the band. The transition between these two regimes is governed by the ratio of  $E - E_j$  to the band width. In Ga(As, P) for  $x \sim 0.035$ ,  $E_X - E_{NX} < 0.2$  eV and the band width  $\sim 3.0$  eV, so that the model presented here is probably accurate for these energies. It should be also noted that this model is very sensitive to the choice of masses (i.e., the band structure within 0.1–0.2 eV of the band edge) as shown in Figs. 2 and 4(a). With the correct choice of masses, therefore, this model may describe the shape, if not the magnitude, of the Green's function at these energies more accurately than a band-structure calculation,<sup>23</sup> which is accurate on a grosser scale.

<sup>1</sup>M. G. Crawford and N. Holonyak, Jr., in *Optical Properties of Solids: New Developments*, edited by B. O. Seraphin (North-Holland, Amsterdam, 1975), Chap. 5.

<sup>2</sup>P. J. Dean, *J. Lumin.* **1/2**, 398 (1970).

<sup>3</sup>R. A. Faulkner, *Phys. Rev.* **175**, 991 (1968).

<sup>4</sup>D. R. Scifres, N. Holonyak, Jr., C. B. Duke, G. G. Kleiman, A. B. Kunz, M. G. Craford, W. O. Groves, and A. H. Herzog, *Phys. Rev. Lett.* **27**, 191 (1971).

<sup>5</sup>D. R. Scifres, H. M. Macksey, N. Holonyak, Jr., R. D. Dupuis, G. W. Zack, C. B. Duke, G. G. Kleiman, and A. B. Kunz, *Phys. B* **5**, 2206 (1972).

<sup>6</sup>C. B. Duke, D. L. Smith, G. G. Kleiman, H. M. Macksey, N. Holonyak, Jr., R. D. Dupuis, and J. C. Campbell, *J. Appl. Phys.* **43**, 5134 (1972).

<sup>7</sup>George G. Kleiman, *J. Appl. Phys.* **47**, 180 (1976).

<sup>8</sup>M. Altarelli, *Phys. Rev. B* **11**, 5031 (1975).

<sup>9</sup>J. J. Coleman, N. Holonyak, Jr., A. B. Kunz, W. O. Groves, D. L. Keune, and M. G. Craford, *Solid State Commun.* **16**, 319 (1975).

<sup>10</sup>D. E. Aspnes, C. G. Olson, and D. W. Lynch, *Phys. Rev. Lett.* **37**, 766 (1976).

<sup>11</sup>D. E. Aspnes, *Phys. Rev. B* **14**, 5331 (1976).

<sup>12</sup>George G. Kleiman and M. F. Decker, *Phys. Rev. B* **17**, 924 (1978).

<sup>13</sup>G. F. Koster and J. C. Slater, *Phys. Rev.* **95**, 1167 (1954).

<sup>14</sup>D. J. Wolford, B. G. Streetman, R. J. Nelson, and N. Holonyak, Jr., *Solid State Commun.* **19**, 741 (1976).

<sup>15</sup>D. J. Wolford, B. G. Streetman, W. Y. Hsu, J. D. Dow, R. J. Nelson, and N. Holonyak, Jr., *Phys. Rev. Lett.* **36**, 1400 (1976).

<sup>16</sup>R. J. Nelson, N. Holonyak, Jr., J. J. Coleman, D. Lazarus, D. J. Wolford, W. O. Groves, D. L. Keune, M. G. Craford, and B. G. Streetman, *Phys. Rev. B* **14**, 685 (1976).

<sup>17</sup>M. G. Craford, R. W. Shaw, A. H. Herzog, and W. O. Groves, *J. Appl. Phys.* **43**, 4075 (1972).

<sup>18</sup>N. Holonyak, Jr., R. D. Dupuis, H. M. Macksey, M. G. Craford, and W. O. Groves, *J. Appl. Phys.* **43**, 4148

- (1972).
- <sup>19</sup>George G. Kleiman, R. J. Nelson, N. Holonyak, Jr., and J. J. Coleman, *Phys. Rev. Lett.* **37**, 375 (1976).
- <sup>20</sup>N. Holonyak, Jr., R. J. Nelson, J. J. Coleman, P. D. Wright, D. Finn, W. O. Groves, and D. L. Keune, *J. Appl. Phys.* **48**, 1963 (1977).
- <sup>21</sup>N. Holonyak, Jr. (unpublished).
- <sup>22</sup>George G. Kleiman, *Phys. Rev. B* **15**, 802 (1977).
- <sup>23</sup>W. Y. Hsu, J. D. Dow, D. J. Wolford and B. G. Streetman, *Phys. Rev. B* **16**, 1597 (1977).
- <sup>24</sup>J. M. Ziman, *Principles of the Theory of Solids* (Cambridge University, London, 1964).
- <sup>25</sup>J. M. Luttinger and W. Kohn, *Phys. Rev.* **97**, 869 (1955); C. Kittel and A. H. Mitchell, *ibid.* **96**, 1488 (1954); W. Kohn and J. M. Luttinger, *ibid.* **98**, 915 (1955); W. Kohn, *Solid State Phys.* **5**, 257 (1957).
- <sup>26</sup>George G. Kleiman and M. F. Decker (unpublished).
- <sup>27</sup>R. J. Nelson, N. Holonyak, Jr., J. J. Coleman, D. Lazarus, D. L. Keune, A. H. Herzog, W. O. Groves, and G. G. Kleiman, *Appl. Phys. Lett.* **29**, 615 (1976).
- <sup>28</sup>J. Chevallier, H. Mariette, D. Diguët and G. Poibland, *Appl. Phys. Lett.* **28**, 375 (1976).
- <sup>29</sup>R. S. Bauer, Proceedings of the Autumn School on Modulation Spectroscopy, Sunny Beach, Bulgaria, September 27, 1976 (unpublished).
- <sup>30</sup>R. S. Bauer, D. R. Scifres, and R. D. Burnham, Proceedings of the Thirteenth International Conference on the Physics of Semiconductors, Rome, Italy, August 30–September 3, 1976 (unpublished), p. 1286.
- <sup>31</sup>In Ref. 23, the term coupling the symmetric states arising from the nearest-neighbor shell and the nitrogen cell was observed to be small and was neglected. The two states were fit independently to  $N_{\Gamma}$  and  $N_X$ , respectively. The strong influence which the small coupling term exerts on the Green's functions, which vary slowly in energy, reflects our comments on the interdependence of the solutions and, in this model, makes it impossible to fit the full solution to the data.
- <sup>32</sup>S. F. Ross and M. Jaros, *J. Phys. C* **10**, L51 (1977).
- <sup>33</sup>In Sec. II A especially, we draw on results derived in Ref. 23 (and cite appropriately) because the contexts are similar.
- <sup>34</sup>J. Callaway, *J. Math. Phys.* **5**, 783 (1964).
- <sup>35</sup>M. Lax, *Symmetry Principles in Solid State and Molecular Physics* (Wiley, New York, 1974); M. I. Petrashen and E. D. Trifonov, *Applications of Group Theory in Quantum Mechanics* (MIT, Cambridge, Mass., 1969); M. Tinkham, *Group Theory and Quantum Mechanics* (McGraw-Hill, New York, 1964).
- <sup>36</sup>We denote this representation by  $\Gamma_1$  instead of the representation dependent label  $A_1$  to indicate that there is a one-to-one compatibility relation between the  $\Gamma_1$  of  $T_d$  and of all its subgroups.
- <sup>37</sup>These results can be immediately cited from the matrix orthogonality theorem (see Ref. 35) but probably require more notation of definitions than present derivation. Although Eq. (4c) can be derived from the symmetry properties at  $k=0$ , it may be worthwhile to present this derivation in the present context.
- <sup>38</sup>In discussing photoluminescence data, however, these states should be taken into account in order to describe transfer of electrons from the conduction band in radiative as well as nonradiative processes.
- <sup>39</sup>G. F. Koster, J. O. Dimmock, R. G. Wheeler, and H. Statz, *Properties of the Thirty-two Point Groups* (MIT, Cambridge, Mass., 1963).
- <sup>40</sup>A. Onton and R. C. Taylor, *Phys. Rev. B* **1**, 2587 (1970); C. Alibert, G. Bordure, A. Laugier, and J. Chevallier, *ibid.* **6**, 1301 (1972).
- <sup>41</sup>D. Bohm, *Quantum Theory* (Maruzen, Tokyo, 1951); L. D. Landau and E. M. Lifshitz, *Quantum Mechanics* (Pergamon, London, 1958).
- <sup>42</sup>J. M. Ziman, *Elements of Advanced Quantum Theory* (Cambridge University, Cambridge, England, 1969).
- <sup>43</sup>It is possible to have a nondecreasing intermediate-range potential (i.e., which is nonlocal in  $\vec{k}$  space) whose range is greater than that of the square-well potential to which the effective-mass approximation is applicable (i.e., 20–25 Å). Obviously, the distinction between intermediate and long range becomes blurred in this case.
- <sup>44</sup>T. N. Morgan and H. Maier, *Phys. Rev. Lett.* **27**, 1200 (1971).
- <sup>45</sup>A. Baldereschi, in *Proceedings of the International Symposium at Pugnochiuso, Italy, Sept. 4–10, 1972*, edited by A. Froya (North-Holland, Amsterdam, 1973), p. 79.